

MODE Bottom Experiment¹

WENDELL BROWN,² WALTER MUNK,² FRANK SNODGRASS,² HAROLD MOFJELD³
AND BERNARD ZETLER²

(Manuscript received 2 July 1974, in revised form 9 September 1974)

ABSTRACT

Pressure fluctuations on the deep seafloor at frequencies below inertial and tidal have been measured. Between 0.1 and 1 cycle per day the variance is about 2 mb², spectra diminish with increasing frequency as ω^{-n} , $n=1.5$ to 2, and a signal-to-instrument noise ratio of 10 dB is achieved. Fluctuations are in phase and highly coherent within the MODE area (>0.95 at 200 km) and even with inferred (atmosphere plus sea level) Bermuda subsurface pressures (0.8 at 700 km). Station *differences* (to which MODE-sized eddies would make the principal contribution) are relatively small. The large horizontal scale of the recorded bottom pressure fluctuations resembles that of atmospheric pressure, yet the coherence locally between atmospheric and bottom pressure is slight; the recorded fluctuations may be related to a barotropic ocean response to a variable wind stress on the subtropical gyre. Bottom temperature records show "sudden" (1 day) changes of order 30 millidegrees Celcius separated by long intervals (20 days) of uniform temperatures. The changes are much larger than have been observed in the Pacific. They are correlated at horizontal separations of 2 km, but uncorrelated to bottom pressure and to temperatures 1 km above the seafloor.

1. Introduction

Measurements of atmospheric surface pressure go back to the very beginnings of meteorology. When these measurements are referred to some standard level (sea level), it is found that surface winds are directed approximately along isobars with a speed proportional to the horizontal pressure gradient. "Geostrophy" is the term applied to this idealization in the relation (sea level or aloft) between wind and pressure fields.

The corresponding practice (or malpractice) of inferring currents from the pressure field is equally embedded in oceanography, yet an experiment to test the geostrophic "law" using direct pressure measurements has not been previously attempted. Accordingly, the Bottom Experiment Subcommittee (J. Baker, Chairman) of the Mid-Ocean Dynamics Experiment (MODE) planned for an array of bottom pressure recorders, to be closely coordinated with measurements of currents and the density field. There was never any question of referring pressures to some common level (following meteorological practice); differences in the elevation of the various instruments are not known to anywhere near the required precision. The goal was to measure *variations* in the pressure differences between

stations, for comparison with corresponding variations in currents.⁴

The experiment was considered marginal from the outset. Surface atmospheric pressure can vary by a few percent; geostrophic bottom fluctuations⁵ by some millibars represent a fractional change of only a few parts in 10⁶. The geostrophic fluctuations are small compared to the tidal variations at higher frequency (the reverse holds for surface atmospheric pressure). The chief difficulty, however, is not a lack of instrument sensitivity, nor the removal of high-frequency tidal components (nor even the relative remoteness of the seafloor), but rather the instrumental noise at low frequencies, i.e., *drift*. In this connection the longer oceanic time scales (months compared to days) adds to the difficulties.

With the very reality of signals in doubt, emphasis was placed on redundancy rather than spatial coverage. And this was indeed a wise choice. It demonstrated that we did, in fact, succeed in measuring geostrophic (sub-inertial) bottom pressure fluctuations, but that the relatively small station *differences* were only marginally above instrument noise level and not adequate to test "geostrophy." The results are not those we anticipated

¹ MODE Contribution No. 15.

² Institute of Geophysics and Planetary Physics, Scripps Institution of Oceanography, University of California, La Jolla 92037

³ Atlantic Oceanographic and Meteorological Laboratories, NOAA, Miami, Fla. 33124

⁴ As stated succinctly by a reviewer, if we write $A = \rho^{-1} \partial p / \partial x - fv = 0$, classical oceanography considers $\partial A / \partial z$, while the present experiment is concerned with $\partial A / \partial t$.

⁵ Throughout this paper, "geostrophic fluctuation" refers to any fluctuation at frequencies small compared to the inertial frequency.

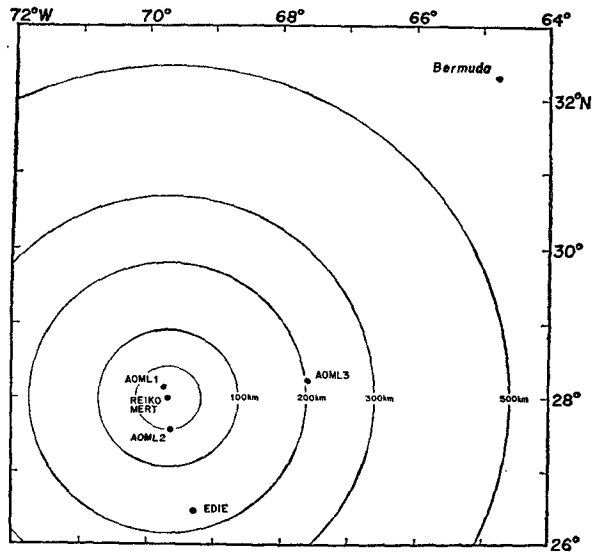


FIG. 1. MODE bottom pressure stations: AOML (1, 2, 3) and IGPP (EDIE, MERT, REIKO). REIKO and MERT were 2 km from the central mooring (28°00' N, 69°40' W).

(as is so often the case in an oceanographic experiment), but that does not make them any less interesting.

2. Measurements

The AOML⁶ deployment consisted of three stations (Fig. 1) of which AOML 1 and AOML 3 produced useful time series of bottom pressure. Each station involved the deployment and recovery of a Gulf/GA pressure gauge by the NOAA ship *Researcher*. The Filloux Bourdon tube transducer in each gauge experienced creep, resulting in an apparent instrumental drift in pressure of about 430 mb. This drift, rapid at first and then slowing with time, follows a logarithmic law and has been removed from the AOML pressure records.

The IGPP deployment consisted of three cruises: installation, monitoring and repair, and recall. Prior to the MODE deployment, there had been extensive laboratory tests and a series of Pacific drops. All this is discussed in gruesome detail by Snodgrass *et al.* (1975). For the present purpose we note that there is no attempt to remove drift; after the initial day or two this is small (of the order 1 mb per month), but still the limiting factor for measuring pressure differences between stations. Pressures and temperatures were both measured by crystal gauges, and pressure records were corrected for temperature (corrections are only of the order 0.1 mb). But the temperature series are of some independent interest, and we shall describe them briefly.

⁶ The following abbreviations are used throughout: AOML, Atlantic Oceanographic and Meteorological Laboratories; IGPP, Institute of Geophysics and Planetary Physics; NOAA, National Oceanographic and Atmospheric Administration.

3. Bottom temperatures

The principal results are summarized in Figs. 2 and 3. Records are characterized by "sudden" (1-day) changes of the order of 30 millidegrees Celsius ($m^{\circ}C$) separated by long intervals (20 days) of uniform temperatures (within 5 $m^{\circ}C$). The corresponding instrumental noise is of order 1 $m^{\circ}C$ (Snodgrass *et al.*, 1975).

Month-to-month changes cannot be detected, as they are less than instrumental drift (0.5 $m^{\circ}C$ in two months). Measurements at REIKO and MERT (Fig. 1) (separated by 2 km at the central mooring) exhibit reproducible features, with lags of the order of 1 day. There is no correlation with EDIE 180 km to the south. The fluctuations are larger by a factor of 10 than those we measured in the Pacific, and almost certainly related to the presence of Antarctic Bottom Water.

There is no resemblance to bottom pressure, nor to temperatures measured 1 km above the sea bottom. The latter are the result of vertical displacement (by several hundred meters!) from internal waves and geostrophic fluctuations (Brown, 1975).

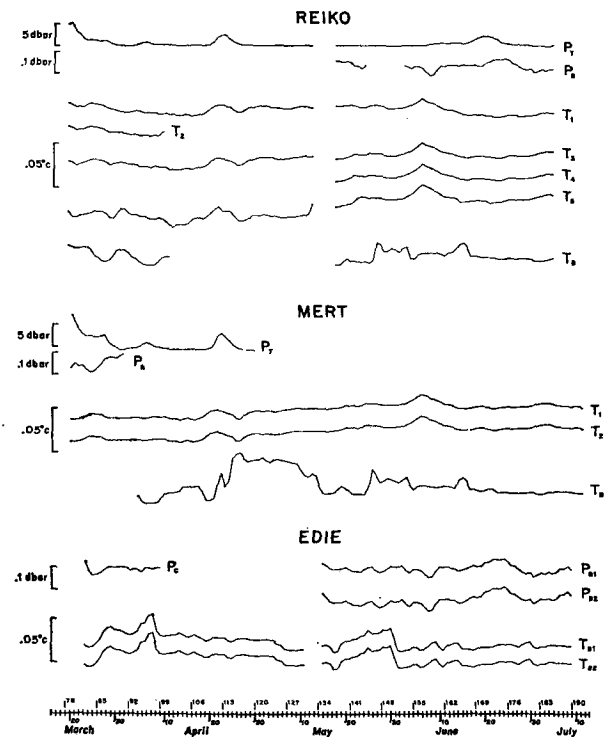


FIG. 2. Summary of low-passed 1973 IGPP MODE pressure and temperature records plotted at 20 h intervals [see Snodgrass *et al.* (1975) for the "raw" records]. P_B and T_B refer to bottom pressures and temperatures, P_T to pressure at the top of a 1 km cable (an indication of cable tilt), and T_1, T_2, \dots , refer to temperatures at the upper end of the cable. EDIE has duplicate pressure and temperature instrumentation on the sea bottom, none aloft; P_C is a composite of P_{B1} and P_{B2} (both of which were noisy). REIKO and EDIE were recovered, repaired and relaunched in mid-May. All temperatures are plotted to the same scale.

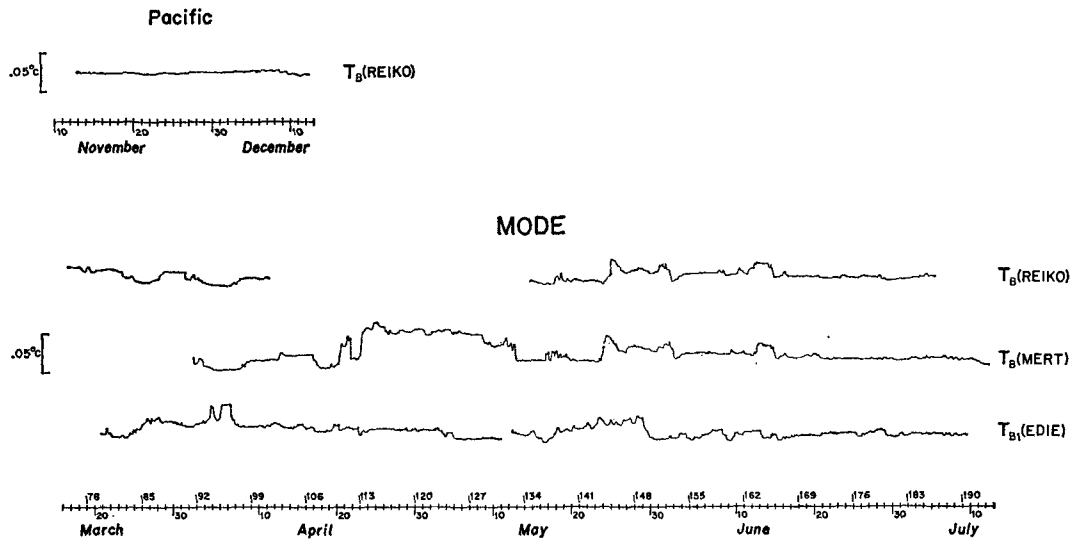


FIG. 3. Bottom temperatures at REIKO and MERT (separation 2 km) and EDIE (separation 170 km). For comparison, a typical Pacific record (REIKO 250 SW; Snodgrass *et al.*, 1975) is shown on the same scale. In contrast to Fig. 2, the records have not been low-passed, and are plotted at 24-min intervals.

4. Bottom pressures

Tides were removed by subtracting the “response predicted” deep-sea tides, with Bermuda-predicted tides taken as reference (Zetler *et al.*, 1975). There is no significant tidal residual in the “detailed” records. For good measure, the detided time series of 45 s averages were low-passed with a 40 dB reduction at 1 cycle per day (cpd) (Fig. 4), and plotted at 24 h intervals (Fig. 5).

Three instruments within 15 km of the central mooring, AOML 1 (a Filloux Bourdon tube), MERT and REIKO (quartz crystals), show a strong resemblance during times of overlapping records. Pressure changes are larger and more sudden than we had suspected; they can amount to 5 mb in a few days. An unexpected result is the resemblance with the distant MODE stations EDIE and AOML 3. Evidently the bottom pressure fluctuations have larger horizontal scales than typical MODE eddies.

We have also plotted atmospheric pressures in the MODE and Bermuda areas,⁷ and these are clearly coherent. In order to learn whether bottom pressures in the two areas are similarly related, we define the “subsurface pressure” (at a fixed point)

$$SSP = p_{atm} + \rho g \eta,$$

where η is the recorded sea level (detided). For a homogeneous ocean the subsurface and bottom pressure

⁷ Mr. Frank Marks, Dept. of Meteorology, MIT, compiled the series of daily atmospheric pressures in the MODE area from weather maps and MODE ships’ microbarograph data. Hourly values of atmospheric pressure were provided by the Environmental Data Service, NOAA, Ashville, N. C.; values of Bermuda sea level were provided by the National Ocean Survey, NOAA, Rockville, Md.

should be the same, and this is nearly the case for the *barotropic* response of a stratified ocean (see Appendix). For *baroclinic* waves of odd order, including the gravest mode, subsurface and bottom pressures (aside from atmospheric effects) are of equal amplitude but in anti-phase. We regard the resemblance between Bermuda subsurface and MODE bottom pressures as an indication for a predominantly barotropic response. Further, island interference is evidently not a major consideration. As we shall find, the SSP emerges as a useful index whose interpretation is quite distinct from that of its two components, atmospheric pressure and sea level.

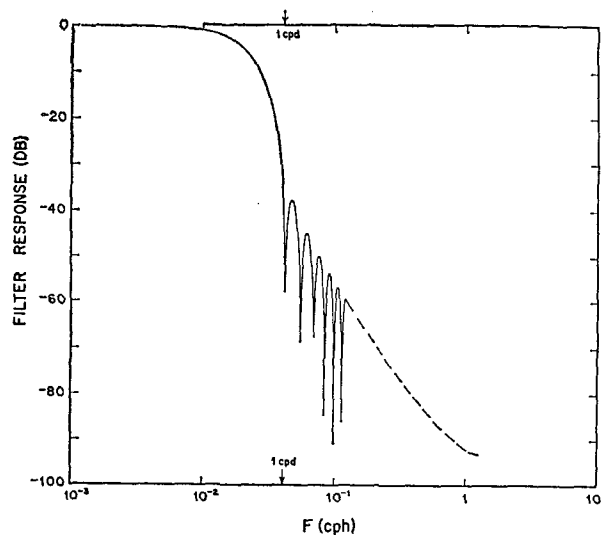


FIG. 4. Low-pass filter applied to MODE records. The energy rejection at 1 cpd is 40 dB.

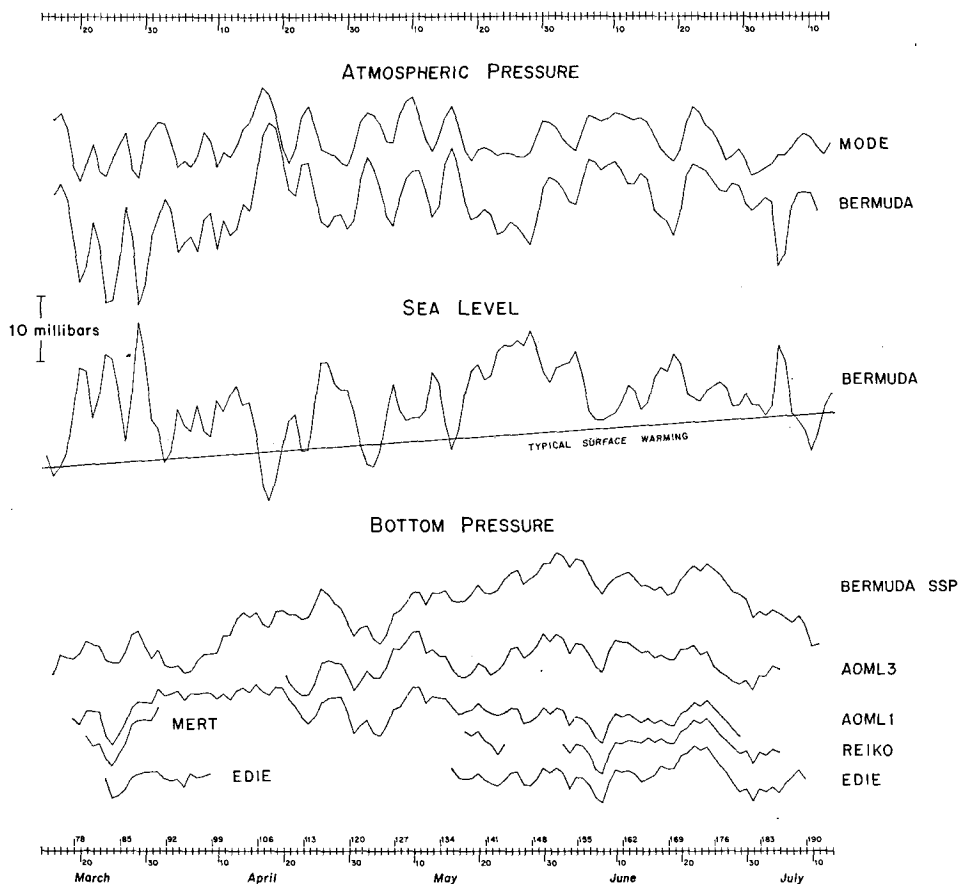


FIG. 5. Atmospheric pressure at Bermuda and in the MODE area, Bermuda sea level (detided, and in equivalent pressure units), Bermuda subsurface pressure (atmospheric plus equivalent sea level), and various MODE recorded bottom pressures. All plots to the same scale. Dates and year days are indicated. Tick marks are Greenwich midnight.

To a good approximation the components cancel in accordance with the “inverted barometer” response.

A superimposed upward drift in $\rho g \eta$ and hence SSP, which is not found in the MODE bottom pressures, can reasonably be ascribed to thermal expansion from seasonal warming of Bermuda surface waters; if so, this would not be associated with any change in the mass per unit area, or resulting bottom pressure.

5. Spectral estimates

We now attempt to lend these qualitative remarks some semblance of the magnitudes involved. Spectra of Bermuda subsurface and observed MODE bottom pressures are in accord (Fig. 6). The rise centered at 0.35 cpd is consistent with the behavior of atmospheric pressure spectra (Fig. 7). Atmospheric pressure spectra are higher by a factor of 5 than those on the seafloor.

MODE bottom spectra are significantly coherent (except at the lowest frequency) among one another (Fig. 8), and with respect to Bermuda subsurface pressure. MODE and Bermuda atmospheric pressures

are highly coherent, as expected (Fig. 9). MODE bottom pressures somewhat lag Bermuda subsurface pressures, whereas the opposite holds for atmospheric pressure. Bermuda sea level and atmospheric pressure are highly coherent and out of phase (Fig. 10). On the other hand, bottom and local atmospheric pressures are barely coherent, and show no fixed phase relation. A summary of the statistical analyses is presented schematically in Fig. 11. All of the evidence points toward something other than local atmospheric pressure for the source of the bottom pressure fluctuations. This inference will be examined in the light of a simple model.

6. Model

We follow the analysis by Munk and Bullard (1963). Let

$$p_1 = a \cos(\omega t + \alpha)$$

$$p_2 = r a \cos(\omega t + \alpha) + s a \sin(\omega t + \alpha) + x(t) = \bar{\rho} g \eta$$

$$p_3 = p_1 + p_2 = (1+r)a \cos(\omega t + \alpha) + s a \sin(\omega t + \alpha) + x(t)$$

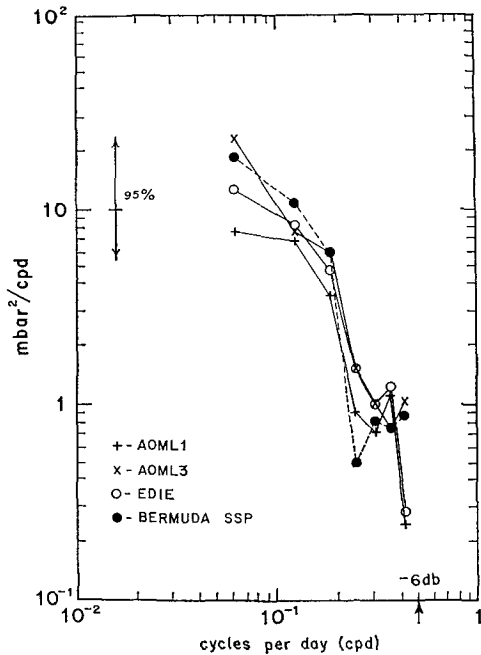


FIG. 6. Spectra of bottom pressure fluctuations for MODE (solid) and Bermuda (dashed) (16 degrees of freedom). Frequencies above those plotted are significantly reduced by numerical filtering (-6 dB at 0.5 cpd).

designate atmospheric, sea-level and bottom pressures within a narrow frequency band centered on ω ; $a(t)$ and $\alpha(t)$ are slowly varying (compared to ω) amplitude and

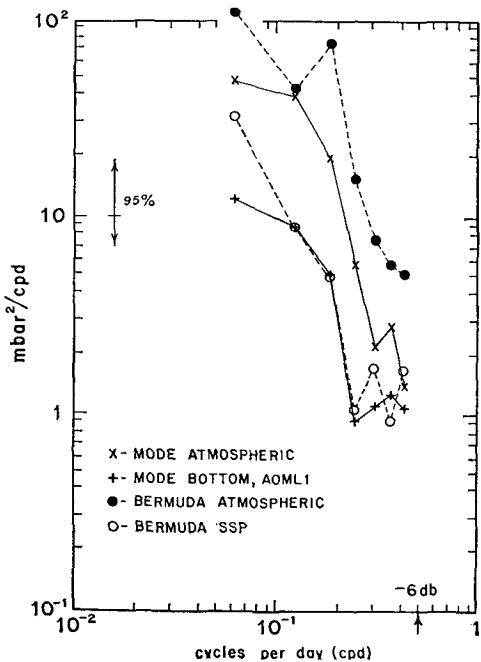


FIG. 7. Comparative spectra of atmospheric and bottom pressures (34 degrees of freedom) for MODE (solid) and Bermuda (dashed).

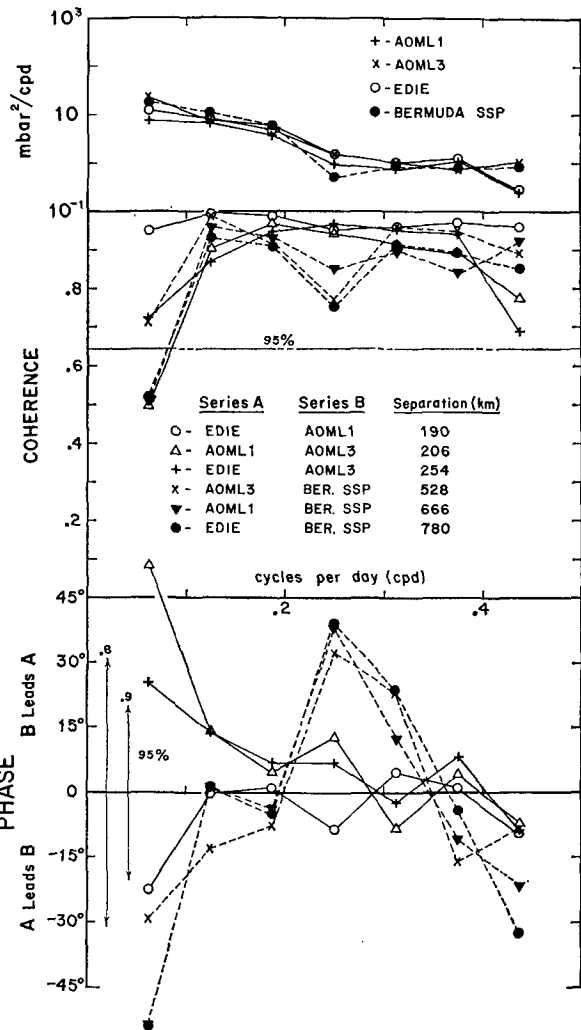


FIG. 8. Cross spectra for MODE pressures and Bermuda sub-surface pressures (all spectra and cross spectra involving Bermuda are dashed). Degrees of freedom are 16; the 95% significance level for coherence (not squared), and the 95% phase uncertainties for 0.8 and 0.9 coherences are indicated.

phase. We interpret $\langle \frac{1}{2} a^2 \rangle$ as the spectral energy in the band $\omega \pm \frac{1}{2} \delta \omega$. $x(t)$ is that portion of p_2 and p_3 which is uncorrelated to p_1 , i.e.,

$$\langle p_1(t)x(t-\tau) \rangle = 0.$$

Then by performing the appropriate lagged covariances and Fourier transforms, it follows that

$$\begin{aligned} S_{11} &= \langle \frac{1}{2} a^2 \rangle \\ S_{22} &= [r^2 + s^2] S_{11} + S \\ S_{33} &= [(1+r)^2 + s^2] S_{11} + S \\ C_{12} &= r S_{11}, \quad Q_{12} = s S_{11} \\ C_{13} &= (1+r) S_{11}, \quad Q_{13} = s S_{11} \end{aligned}$$

are the spectra, co- and quadrature spectra, respectively, with $S(\omega)$ the spectrum of $x(t)$. S_{22} and S_{33} are

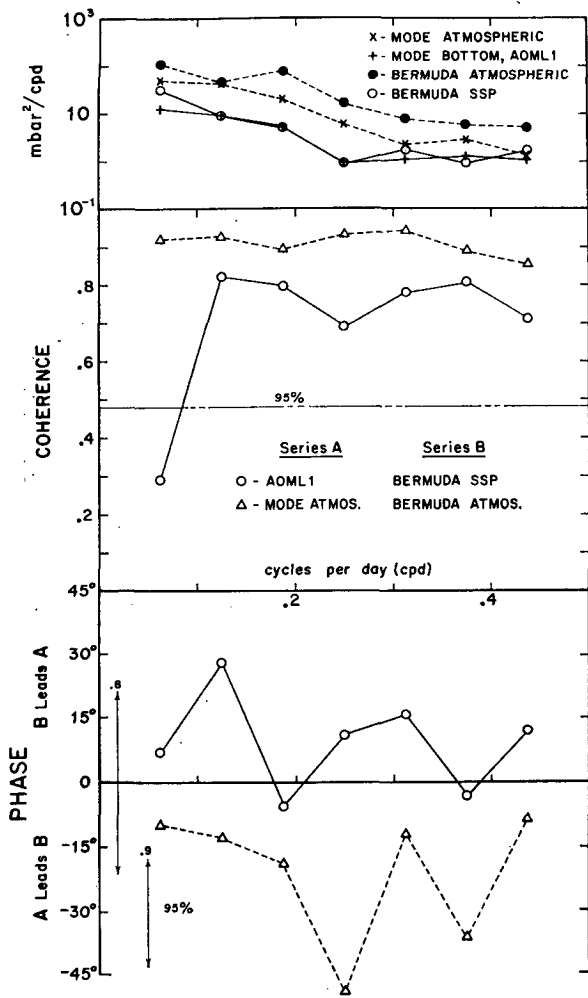


FIG. 9. Cross spectra of MODE vs Bermuda atmospheric pressure (dashed) and MODE vs Bermuda subsurface pressures (34 degrees of freedom). The 95% phase uncertainties are drawn for 0.8 and 0.9 coherences.

written as the sum of two terms: the first is coherent with atmospheric pressure, the second (S) is incoherent. For an inverted barometer's response⁸

$$r = -1, s = 0: S_{22} = S_{11} + S, S_{33} = S.$$

In terms of coherence R_{ij} and phase ϕ_{ij} ,

$$\begin{pmatrix} C_{ij} \\ Q_{ij} \end{pmatrix} = (S_{ii}S_{jj})^{1/2} R_{ij} \begin{pmatrix} \cos \phi_{ij} \\ \sin \phi_{ij} \end{pmatrix},$$

$$r = R_{12} \cos \phi_{12} (S_{22}/S_{11})^{1/2}, \quad s = R_{12} \sin \phi_{12} (S_{22}/S_{11})^{1/2},$$

$$S = (1 - R_{12}^2) S_{22}, \quad S_{33} = S_{22} + (2r + 1) S_{11}.$$

These formulas permit the calculation of r, s, S, S_{33} from the measured $S_{11}, S_{22}, R_{12}, \phi_{12}$ (the cross spectrum of atmospheric pressure and sea level). Fig. 12 has been

⁸ This interpretation has to be qualified if winds make a significant contribution that is coherent with atmospheric pressure.

so constructed, leaning on Wunsch's (1972) Bermuda analysis for the low frequencies, and the MODE observations at the central and high frequencies.

With regard to S_{22} at the central frequencies, this nearly equals $(r^2 + s^2)S_{11}$, the contribution coherent with atmospheric pressure. Since the inverted barometer (IB) condition nearly holds, $S_{22} \approx S_{11}$. (See Appendix for a discussion of the IB condition.) The incoherent contribution S is smaller by an order of magnitude. This is not the case at very high and low frequencies, where $S \gg S_{11}$ and $S_{22} \rightarrow S_{33}$. Evidently the predominance of S_{22} over S_{33} at central frequencies is related to a change in slope of the S_{11} spectrum.

With regard to S_{33} the situation is different, and the principal contribution comes from S at all frequencies. We will not attempt here to identify the incoherent spectrum S with any specific geophysical process; the large horizontal scale suggests an atmospheric process, and the coherence found by Wunsch between Bermuda

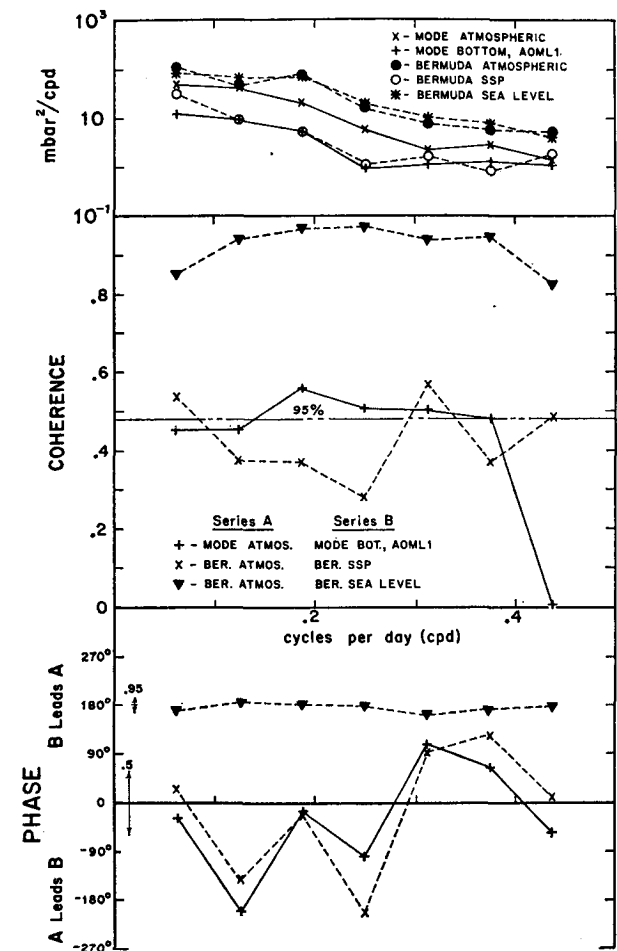


FIG. 10. Cross spectra of bottom pressures and Bermuda sea level vs local atmospheric pressures (34 degrees of freedom). Bermuda spectra are dashed. Phase uncertainties are shown for 0.95 and 0.5 coherences.

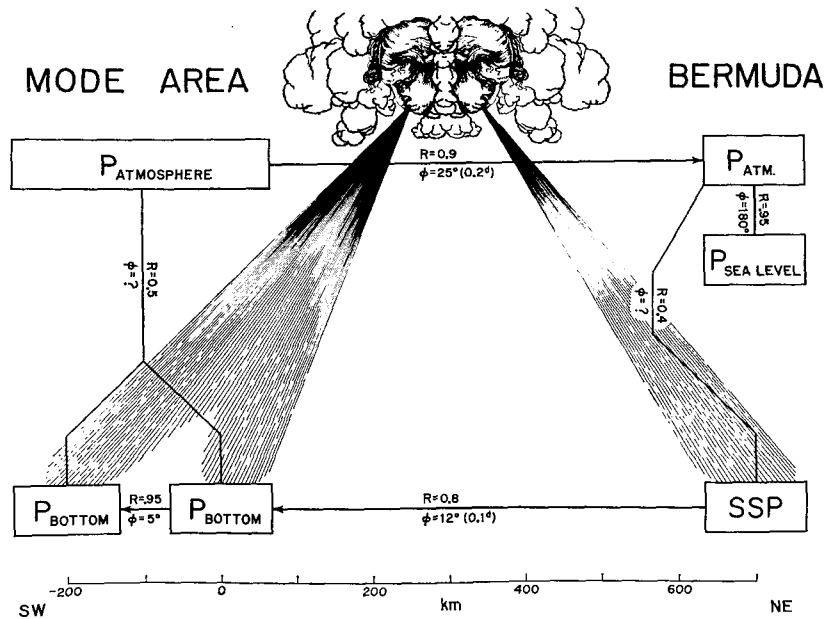


FIG. 11. Schematic presentation of coherences R and phases ϕ (in direction of arrows) in the 0.1–0.5 cpd frequency band. Atmospheric pressures (or SSP) are highly coherent over the MODE area and between MODE and Bermuda, as are MODE bottom pressures and MODE bottom pressure with Bermuda SSP; but the local coherences between atmospheric and bottom pressure (or SSP) are very low. Some common and unknown source of the MODE and Bermuda bottom pressures is indicated.

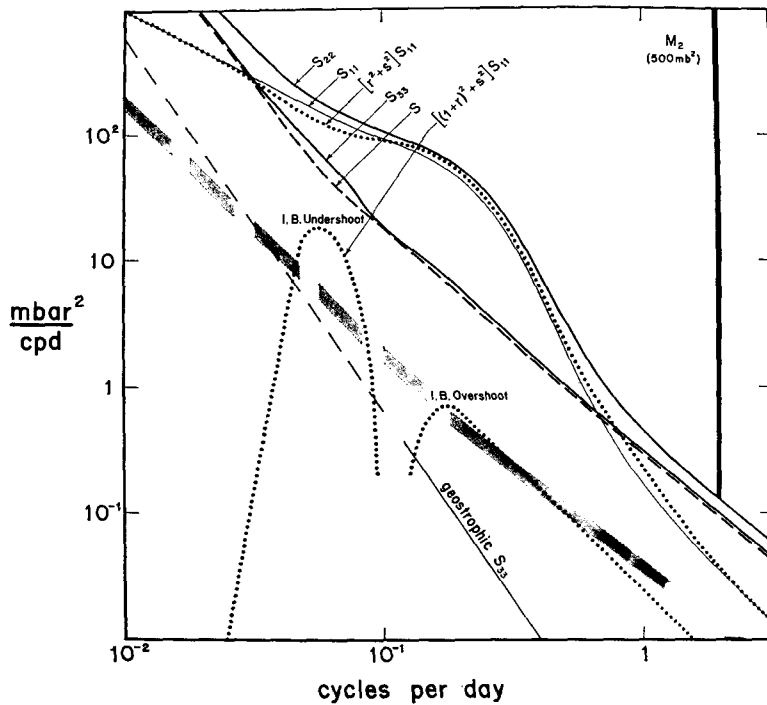


FIG. 12. Idealized spectra of atmospheric pressure (S_{11}), sea level (S_{22} , in equivalent pressure units) and bottom pressure (S_{33}). $[r^2 + s^2] S_{11}$ and $[(1+r)^2 + s^2] S_{11}$ are the contributions to S_{22} and S_{33} , respectively, that are coherent with atmospheric pressure; S is the noncoherent contribution to both S_{22} and S_{33} . Bottom pressures inferred from MODE bottom velocity measurements are designated "geostrophic S_{33} ," and lie below the noise spectrum of bottom pressure transducers (inferred from duplicate instrumentation); extrapolation from 0.1 to 0.01 cpd is uncertain.

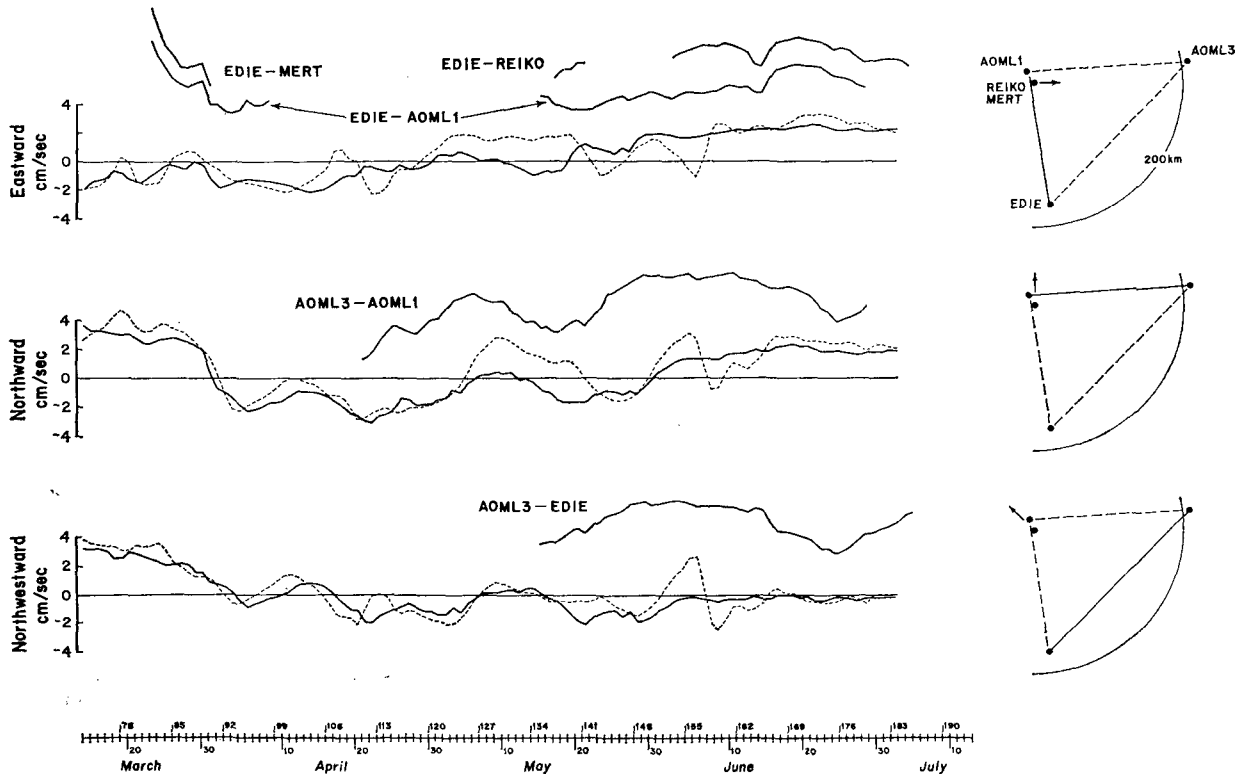


FIG. 13. Components of measured bottom currents (depth 5356 m, dashed) and deep currents (3963 m, solid) at central mooring. For comparison, fluctuations in currents inferred geostrophically from pressure differences between stations are plotted to the same scale, but with arbitrary zero offset.

sea level and local winds (Figs. 8 and 10 of Wunsch, 1972) is certainly suggestive. The analysis by Phillips (1966) leads to a reasonable magnitude: $rms(p_3) = (L/h) rms(\tau)$, where p_3 and τ are bottom pressure and surface stress, and $L/h = 5000 \text{ km}/5 \text{ km}$ is the ratio of the horizontal stress scale to ocean depth (Appendix). For $\tau = 1 \text{ dyn cm}^{-2}$, $p_3 = 10^3 \text{ dyn cm}^{-2} = 1 \text{ mb}$.

At 0.1 cpd the IB condition is taken to be exactly fulfilled, and S is the sole contribution to S_{33} ; at other frequencies there is an additional slight $[(1+r)^2 + s^2] S_{11}$ contribution to S_{33} because of the departure from the IB condition: an IB undershoot below 0.1 cpd, an IB overshoot above 0.1 cpd. If we take $1+r$, s and $1-R_{12}$ as small and all of order ϵ , then the relative magnitude in the coherent and incoherent (with atmospheric pressure) contributions to sea level and sea bottom spectra is as follows:

	Coherent	Incoherent
Sea level	1	ϵ
Sea bottom	ϵ^2	ϵ

7. Discussion

Bottom and deep currents at the MODE central mooring⁹ are plotted in Fig. 13, together with the

⁹ We are grateful to the Woods Hole Oceanographic Institution for having made the records available.

geostrophic currents computed from station differences. There is a resemblance in the northward components at low frequencies (currents 1400 m above the seafloor are better correlated than bottom currents). The "geostrophic" spectrum in bottom pressure has been estimated from the bottom velocity spectrum, using a factor

$$\langle p_3^2 \rangle / \langle v^2 \rangle = (10^{-3} \rho f / k)^2 = (0.4 \text{ mb cm}^{-1} \text{ s}^{-1})^2$$

for typical MODE eddies ($k = 2\pi/\lambda = 2\pi/350 \text{ km}$, $f = 6.8 \times 10^{-5} \text{ s}^{-1}$). This lies far beneath the observed S_{33} , and also below the instrumental noise figure by Snodgrass *et al.* (1975), except perhaps at very low frequencies (Fig. 12). This is related to the fact that the difference between two instruments placed side by side is of the same order as the station difference (Fig. 14).

Bottom pressure and velocity fluctuations (rms) can now be estimated as follows:

	0.01 to 0.1 cpd	0.1 to 1 cpd
MODE eddies ($\lambda/2\pi = 50 \text{ km}$)	2 mb 5 cm s ⁻¹	0.2 mb 0.5 cm s ⁻¹
Large-scale fluctuations ($\lambda/2\pi = 1000 \text{ km}$)	8 mb 1 cm s ⁻¹	1.5 mb 0.2 cm s ⁻¹

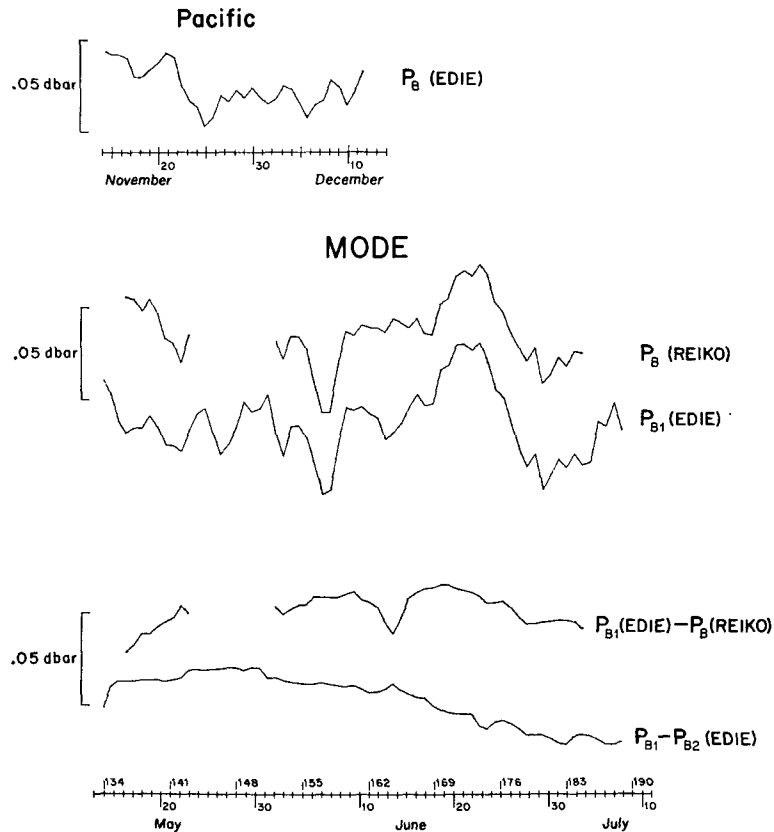


FIG. 14. Some bottom pressures and pressure differences during the latter half of the MODE experiment. The difference $P_{B1} - P_{B2}$ between two pressure sensors on EDIE capsule is of the same order as the difference between capsules EDIE and REIKO separated by 170 km [the negative spike in $P_{B1}(EDIE) - P_B(REIKO)$ on 13 June occurs during a period of excessive instrument noise (Snodgrass *et al.*, 1975)]. For comparison, a Pacific record taken in 1972 is plotted to the same scale.

The large-scale fluctuations have larger pressure variations than the MODE eddies, but because of their much larger horizontal scale, the associated current velocities are relatively small. (On hindsight, this situation might

have been anticipated from an extrapolation of Wunsch's results.) Consequently, the observed bottom pressures are related primarily to the large-scale fluctuations, whereas the observed bottom currents are related mostly to MODE eddies. (Pressure differences between stations would be dominated by MODE eddies, but are only marginally above noise level.) We have succeeded in measuring geostrophic bottom pressures, but failed in testing geostrophy.

Acknowledgments. IGPP work was supported by the Office of Naval Research (Contract N00014-69-A-0200-6008) and the National Science Foundation (Grant NSF-GX-29052). The AOML work was supported under the National Science Foundation agreement AG-253 for NOAA participation in the International Decade of Ocean Exploration.

APPENDIX

Subsurface Pressure

For a free progressive wave in a rotating ocean of constant Väisälä frequency N and depth h , the ratio of

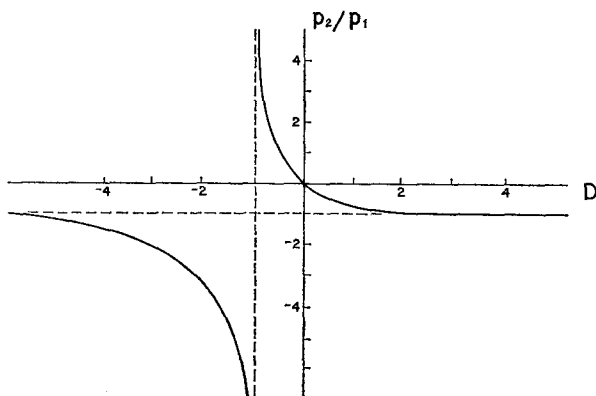


FIG. 15. Response of sea level to atmospheric pressure: $p_2/p_1 = -1$ for inverted barometer response.

subsurface pressure $\rho_0 g \eta$ to bottom pressure is given by (Munk and Phillips, 1968, p. 450)

$$SSP/p_b = \cos(Nh/C),$$

with

$$\tan(Nh/C) = CN/g$$

serving as a definition for C (the phase speed in a non-rotating system). For barotropic waves, $Nh/C \ll 1$; hence

$$C = \sqrt{gh}(1 + \epsilon^2/6), \quad SSP/p_b = 1 - \frac{1}{2}\epsilon^2,$$

where

$$\epsilon^2 = N^2 h / g = O(\Delta\rho/\rho)$$

is a small number. Subsurface and bottom pressures are nearly the same. For baroclinic waves, $(Nh/C - r\pi) \ll 1$, $r = 1, 2, \dots$,

$$C = \frac{Nh}{r\pi} \left(1 - \frac{\epsilon^2}{r^2\pi^2} \right), \quad SSP/p_b = (-1)^r \left(1 - \frac{\epsilon^4}{2r^2\pi^2} \right).$$

Thus, subsurface and bottom pressures are of very nearly the same amplitude, but out of phase for odd modes.

Inverted Barometer Problem

Let u, v designate eastward and northward velocity components, η the surface elevation, and $p_1 = \rho g \xi$ surface atmospheric pressure. We then have for an ocean of constant depth h and density ρ

$$\left. \begin{aligned} \frac{\partial u}{\partial t} - fv &= -g \frac{\partial}{\partial x} (\xi + \eta) \\ \frac{\partial v}{\partial t} + fu &= -g \frac{\partial}{\partial y} (\xi + \eta) \\ \frac{\partial \eta}{\partial t} &= -h \left(\frac{\partial u}{\partial x} + \frac{\partial v}{\partial y} \right) \end{aligned} \right\},$$

which can be combined into

$$\frac{\partial^2 u}{\partial y \partial t} - \frac{\partial^2 v}{\partial x \partial t} - \beta v + fh^{-1} \frac{\partial \eta}{\partial t} = 0,$$

where $\beta = df/dy$, and f the Coriolis frequency. For frequencies ω small compared to f , we neglect $\partial(u, v)/\partial t$, and

$$\lambda^2 \frac{\partial}{\partial t} \nabla^2 (\xi + \eta) + \beta \frac{\partial}{\partial x} (\xi + \eta) = \frac{\partial \eta}{\partial t},$$

where

$$\lambda = (gh)^{1/2} / f$$

is the Rossby radius of deformation. Assuming cellular oscillations of the type

$$\cos \tilde{l}y \cos(kx - \omega t),$$

we obtain

$$\frac{p_2}{p_1} = \frac{\eta}{\xi} = -\frac{D}{1+D}, \quad D = \lambda^2(k^2 + l^2 + \beta k/\omega).$$

In the limit of large-scale disturbances, $k, l \rightarrow 0$ and $D \rightarrow 0$, $\eta \rightarrow 0$ (frozen surface), and the atmospheric pressure is geostrophically balanced. In the low-frequency limit of eastward/westward waves, $\omega \rightarrow \pm 0$ and $D \rightarrow \pm \infty$, $p_2/p_1 \rightarrow -1$ (inverted barometer), and $u, v = 0$. For $D = -1$,

$$\frac{\omega}{k} = -\frac{\beta}{\lambda^{-2} + k^2 + l^2},$$

which is the (westward) phase velocity of free Rossby waves, and so $\eta \rightarrow \pm \infty$ because of resonance.

The scaling

$$\hat{k}, \hat{l} = \lambda(k, l), \quad \hat{\omega} = \omega/f,$$

is convenient, leading to

$$D = \hat{k}^2 + \hat{l}^2 + (\hat{k}/\hat{\omega})v^{-1/2},$$

with

$$v^{1/2} = 2\Omega a / (gh)^{1/2}$$

a parameter [$O(1)$] familiar from tidal theory. Setting $\lambda = 3000$ km, $\hat{k}, \hat{l} = 5$, $\hat{\omega} = \pm 0.1$, $v^{1/2} = 2.15$ gives $D = 50 \pm 23$, and we expect p_2/p_1 to be within a few percent of unity.

The foregoing analysis applies to an infinite ocean of constant depth. For the "real" ocean one may have to replace $\beta = df/dy$ by a "topographic" β arising from the gross slope and small-scale topography.

Wind Stress

According to Phillips (1966), a variable eastward wind stress

$$\tau_x = \tau_0 \sin(\pi y/L) e^{i\omega t}, \quad -\frac{1}{2}L \leq y \leq \frac{1}{2}L,$$

generates a meridional component of barotropic flow

$$v = \frac{2\tau_0}{\rho h \beta L} \cos\left(\frac{\pi y}{L}\right) e^{i\omega t} V(\xi, \mu),$$

where $L = 5000$ km is the distance between the trade winds and westerlies. V is a complicated function of the distance $\xi = x/L$ from the coast, and of frequency $\mu = \omega/\omega_{\max}$, with $\omega_{\max} = \beta L/2\pi = 2\pi/(5.71 \text{ days})$. V exhibits a series of resonant peaks, but their contributions to $\langle v^2 \rangle$ are secondary in the interval $\mu = 0.2$ to $\mu = 1$ (0.02 to 0.2 cpd), and $V \approx V_0 \mu^{-1}$, $V_0 \approx [\pi^2(1+2\xi)^2+4]^{1/2} \approx 5^{1/2}$ for $\xi = 0.2$. The wavelength $\mu L = \mu \cdot 5000$ km is consistent with the observed scale of pressure coherence.

To obtain rms pressures, multiply by $\rho f/k$ with $k = 2\pi/\mu L$, and replace $\cos(\pi\mu/L)e^{i\omega t}$ by its rms value $\frac{1}{2}$:

$$\text{rms}(p_3) = \frac{V_0 f L}{2\pi \beta L h} \text{rms}(\tau_0).$$

Accordingly, the seafloor pressure spectrum is proportional to the τ_0 spectrum. Numerically, $V_0/2\pi \approx 1$, $f/\beta L \approx 1$ and $L/h \approx 10^3$. Thus rms pressures (mb) are roughly equal to rms stresses (dyn cm^{-2}).

REFERENCES

- Brown, W. S., 1975: MODE internal waves. *J. Phys. Oceanogr.* (in preparation).
- Munk, W. H., and E. C. Bullard, 1963: Patching the long-wave spectrum across the tides. *J. Geophys. Res.*, **68**, 3627-3634.
- , and N. Phillips, 1968: Coherence and band structure of inertial motion in the sea. *Rev. Geophys.*, **6**, 447-472.
- Phillips, N., 1966: Large-scale eddy motion in the western Atlantic. *J. Geophys. Res.*, **71**, 3883-3891.
- Snodgrass, F. E., W. S. Brown and W. H. Munk, 1975: MODE: IGPP measurements of pressure and temperature. *J. Phys. Oceanogr.*, **5**, 63-74.
- Wunsch, C., 1972: Bermuda sea level in relation to tides, weather and baroclinic fluctuations. *Rev. Geophys. Space Phys.*, **10**, 1-49.
- Zetler, B. D., W. H. Munk, H. Mofjeld, W. S. Brown and F. O. Dormer, 1975: MODE tides. Submitted to *J. Phys. Oceanogr.*